

BaTiO₃ Nanotubes-Based Flexible and Transparent Nanogenerators

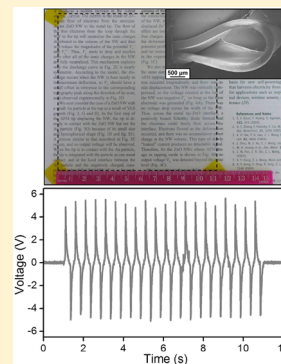
Zong-Hong Lin,[†] Ya Yang,[†] Jyh Ming Wu,[†] Ying Liu,[†] Fang Zhang,[†] and Zhong Lin Wang^{†,‡,*}

[†]School of Material Science and Engineering, Georgia Institute of Technology, Atlanta, Georgia 30332-0245, United States

[‡]Beijing Institute of Nanoenergy and Nanosystems, Chinese Academy of Sciences, China

S Supporting Information

ABSTRACT: We have developed a simple, cost-effective, and scalable approach to fabricate a piezoelectric nanogenerator (NG) with stretchable and flexible characteristics using BaTiO₃ nanotubes, which were synthesized by the hydrothermal method. The NG was fabricated by making a composite of the nanotubes with polymer poly(dimethylsiloxane) (PDMS). The peak open-circuit voltage and short-circuit current of the NG reached a high level of 5.5 V and 350 nA (current density of 350 nA/cm²), respectively. It was used to directly drive a commercial liquid crystal display. The BaTiO₃ nanotubes/PDMS composite is highly transparent and useful for a large-scale (11 × 11 cm) fabrication of lead-free piezoelectric NG.



SECTION: Energy Conversion and Storage; Energy and Charge Transport

Nanogenerators (NGs) that harvest energy from light,¹ mechanical vibration,² and heat³ in the living environment have attracted increasing attention in the past decade. Piezoelectric materials, which can generate electrical charges when mechanically deformed, are the most promising candidates for developing NGs because the source of mechanical energy is ubiquitous and accessible in our living surroundings.⁴ The feasibility of using such type of NGs to power commercial light-emitting diodes (LEDs),⁵ liquid crystal displays (LCDs),⁶ and wireless data transmission⁷ has been demonstrated. Currently, ZnO nanowires are the most outstanding materials for developing NGs due to their unique optoelectronic⁸ and piezoelectric⁹ properties. However, considering the relatively low piezoelectric coefficient of ZnO (12 pC/N),¹⁰ it is desirable to design NGs made by perovskite materials with large piezoelectric coefficients such as BaTiO₃ (100 pC/N)^{11–14} and Pb(Zr,Ti)O₃ (PZT, 200 pC/N)¹⁵ to harvest energy.

NGs fabricated by PZT nanofibers¹⁶ and nanowires¹⁷ have been demonstrated to provide output voltages of 1.63 and 0.7 V, respectively. However, the component lead in PZT has the concern of toxic effect toward human health and environmental problems.¹⁸ Consequently, it has motivated the search for perovskite piezoelectric materials with lead-free properties comparable to PZT with a reduced environmental impact. BaTiO₃ thin-film-based NG fabricated by soft lithographic printing technique can produce an output voltage of 1.0 V and current density of 0.19 μA/cm².¹⁹ Although the above-mentioned result is outstanding, there is no report about using BaTiO₃ nanotubes to fabricate a NG. As the size of the piezoelectric materials is reduced to the nanoscale, the conversion efficiency of mechanical energy has been found to

be improved dramatically, attributing to the larger piezoelectric coefficients and deformations, which are proportional to the generated potential.^{20–22}

In this letter, lead-free BaTiO₃ nanotubes were used to fabricate the piezoelectric NG. A large number of high-quality BaTiO₃ nanotubes were synthesized through a hydrothermal method. By forming a composite of BaTiO₃ nanotubes with poly(dimethylsiloxane) (PDMS) polymer, flexible and transparent NG was developed easily after applying a direct poling process. Under periodic external mechanical deformation by a linear motor, we obtained very stable and high output piezoelectric signals, that is, an open-circuit voltage (V_{oc}) of 5.5 V and short-circuit current (I_{sc}) exceeding 350 nA. The NG was further demonstrated to be easily scaled-up over 11 × 11 cm and can continuously drive a commercial LCD under the biomechanical movements of a human skin.

The NG mainly consists of five layers as schematically shown in Figure 1a. The deposited Au/Cr films act as top and bottom electrodes, and the BaTiO₃ nanotubes and PDMS composite mixed with a 3 wt % ratio serve as the source of piezoelectric potential generation under external stress. The polystyrene (PS) substrate and pure PDMS worked as the supporting and protecting layers to sustain the conformation of NG. Figure 1b shows the cross-sectional scanning electron microscope (SEM) image of a 300 μm thick BaTiO₃ nanotubes/PDMS composite, which demonstrates the flexible property of the developed NG. A transmission electron microscopy (TEM) image depicted in Figure 1c reveals the high purity of BaTiO₃ nanotubes, with

Received: November 6, 2012

Accepted: November 21, 2012

Published: November 21, 2012

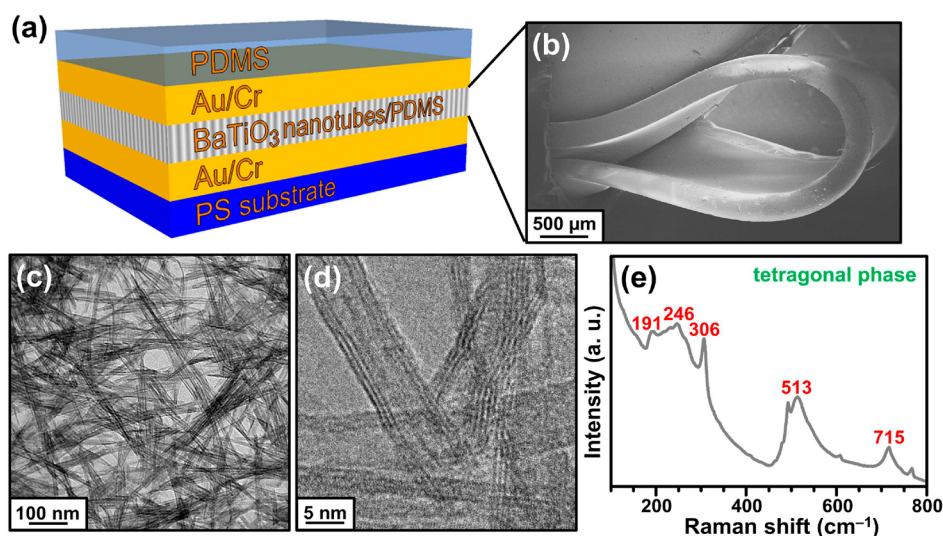


Figure 1. (a) Scheme of the as-developed NG. (b) SEM image of the BaTiO₃ nanotubes/PDMS composite. (c) TEM image of the synthesized BaTiO₃ nanotubes. (d) HRTEM image of the synthesized BaTiO₃ nanotubes. (e) Raman spectrum of the synthesized BaTiO₃ nanotubes.

11.8 (± 2.3) nm in diameter and 4.1 (± 1.2) μm in length. The BaTiO₃ nanotubes were prepared from TiO₂ nanoparticles (P25) and BaCl₂ through a hydrothermal route, with a large-scale preparation and uniform morphology. The BaTiO₃ nanotubes were formed by rolling of BaTiO₃ multisheets (normally three to five layers) with an interlayer distance of ca. 0.8 nm (Figure 1d). The growing mechanism of BaTiO₃ nanotubes is similar to the formation of TiO₂ nanotubes.²³ The high-resolution TEM image (Figure S1a of the Supporting Information) reveals *d* spacing of 0.28 nm for adjacent lattice fringes, which corresponds to the (110) crystalline plane of tetragonal BaTiO₃.²⁴ A typical energy-dispersive X-ray (EDX) analysis of BaTiO₃ nanotubes is displayed in Figure S1b of the Supporting Information, revealing that the atomic ratio of Ba, Ti, and O of the sample is about 19.6:21.3:59.1%.

Figure S1c of the Supporting Information shows the XRD pattern of the as-prepared nanotubes, and the sample has perfectly crystallized perovskite structure, but the tetragonal distortion of BaTiO₃, $\delta = (c - a)/a$, is only 1% in bulk materials, and it is quite difficult to be measured with XRD in nanosized structures for the line-broadening effect.²⁵ The detailed structure information was obtained by Raman spectroscopy (Figure 1e). Cubic BaTiO₃ inherently has no Raman active modes; however, Raman active modes are expected for the noncentrosymmetric tetragonal structure.²⁶ The spectrum of the as-prepared nanoparticles displays bands at 191 cm⁻¹ [A₁(TO), E(LO)], 246 cm⁻¹ [A₁(TO)], 306 cm⁻¹ [B₁, E(TO+LO)], 513 cm⁻¹ [E, A₁(TO)], and 715 cm⁻¹ [A₁, E(LO)], all of which are suggestive of a tetragonal phase.

The typical electrical output of the NG is shown in Figure 2a. The NG was mechanically triggered by a linear motor that provided dynamic impact with controlled force, speed, and frequency. A commercial bridge rectifier was connected to the NG to convert the AC output into DC. For an NG with an effective dimension of 1 cm \times 1 cm, the measured open-circuit voltage (V_{oc}) and short-circuit current (I_{sc}) of the NG could be up to 5.5 V and 350 nA under a stress of 1 MPa, respectively. The high output power of the NG as compared with other reported BaTiO₃-based NGs is because of the small-sized nanotubes. Size-dependent piezoelectricity of BaTiO₃ has been proposed by using a combination of atomistic and theoretical

approaches. An enhancement of 20% of its bulk value at 8 μm and a 500% increase at 5 nm are observed.¹⁹ We found that the generated V_{oc} is proportional to the strength of applied stress. (See Figure S2 of the Supporting Information.) At the stress values of 0.2 and 0.6 MPa, the generated V_{oc} are estimated to be 1.0 and 3.1 V, respectively. We also measured the output of the NG with a reverse connection to the external circuit. The generated V_{oc} and I_{sc} showed the corresponding opposite value in Figure 2b, indicating that the measured signals were generated by the NG. To confirm further that the obtained signal comes from the piezoelectricity of BaTiO₃ nanotubes, we compared the generated V_{oc} with/without the poling progress at ambient temperature by applying an electric field of 80 kV/cm for 12 h. (See Figure S3 of the Supporting Information.) We observed negligible signals for the device without any electric poling because the electric field can help the electric dipoles of the randomly oriented nanotubes inside the PDMS polymer to align along fixed direction.²⁷ The content of BaTiO₃ nanotubes is also important to the fabrication of NG. (See Figure S4 of the Supporting Information.) We found that increasing the ratio of BaTiO₃ nanotubes/PDMS could help to raise the generated V_{oc} of NG; however, too many BaTiO₃ nanotubes within the same region of PDMS will screen the applied stress on each nanotube.

The working mechanism of the NG can be described by the transient flow of inductive charges driven by the piezopotential.²⁸ For simplification of the simulation, a nanowire with similar dimension of the as-prepared nanotube is taken as the model. When the nanowire is subject to a compressive stress, a piezopotential field is created along the nanowire as depicted in Figure S1d of the Supporting Information. As a result of electrostatic force, positive and negative charges will be accumulated at the top and bottom electrodes, which are the flowing charges through an external load. Once the stress is released, the piezoelectric potential should be diminished and the accumulated charges will move back to the opposite direction. In addition, we calculated the piezopotential distributions inside the NG by using a simple rectangular model established by COMSOL software, as described in Figure 2c. The calculated results predict an inductive potential difference of 6 V across the two electrodes at an applied stress

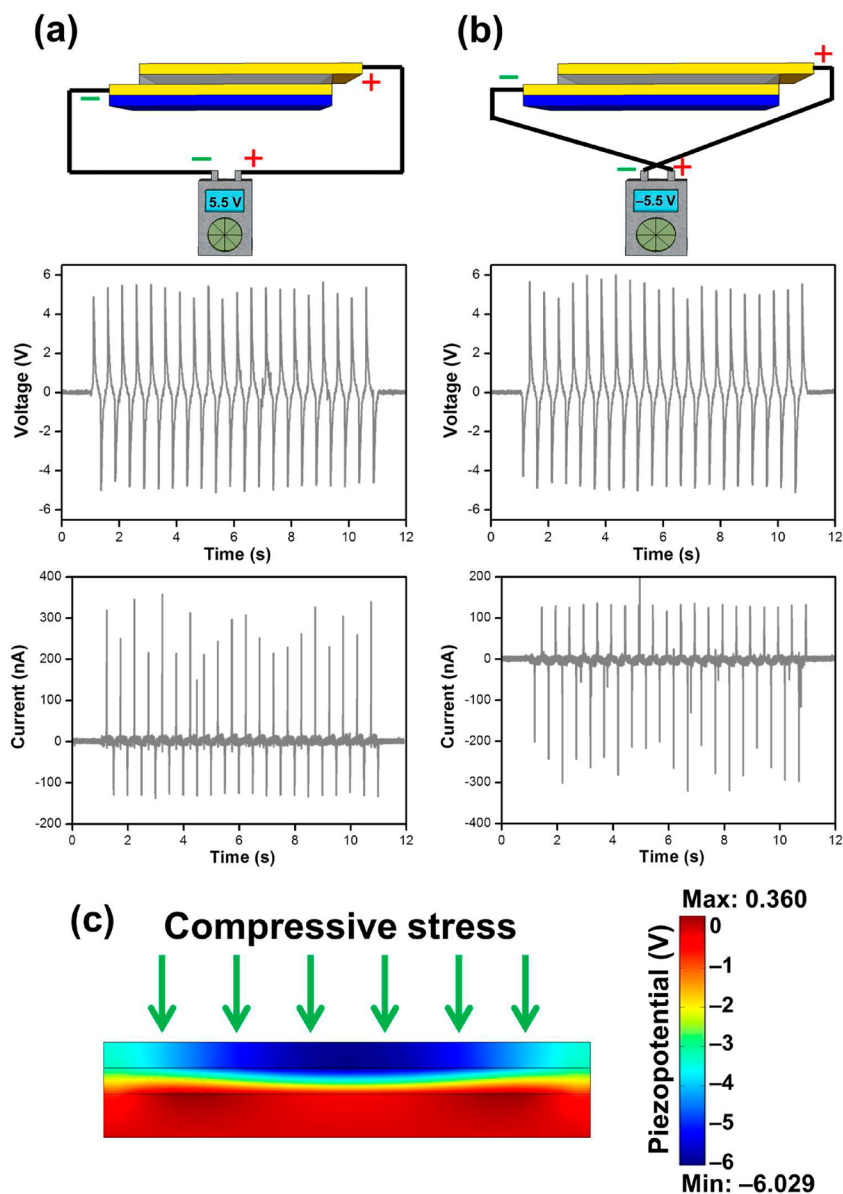


Figure 2. Generated V_{oc} and I_{sc} of the as-developed NG under a compress stress of 1 MPa at forward connection (a) and reversed connection (b) to the measurement system. (c) Demonstration of the working principle of the NG and COMSOL simulation result of the piezopotential in the NG. The simulation is based on a three-layer structure comprised of a top PDMS (300 μm), a layer of BaTiO₃ (300 μm), and a bottom PS substrate (500 μm). The size of the unit cell for calculation is 1 \times 1 cm.

of 1 MPa, which is closed to the measured V_{oc} of the NG. The nonuniform distribution of piezopotential is due to the existence of shear strain in the finite geometry of the NG and the boundary condition.

The potential of the as-developed NG was evaluated by integrating two different devices. The generated V_{oc} of a single nanogenerator for NG nos. 1 and 2 can reach 5.5 and 5.2 V, respectively. (See Figure 3a.) The generated I_{sc} of NG nos. 1 and 2 can exceed 350 and 290 nA, respectively. (See Figure 3b.) By integrating two NGs in serial connection, the generated V_{oc} can exceed 10 V. The generated I_{sc} of NG nos. 1 and 2 in parallel connection can reach 590 nA. These data clearly demonstrate that the generated V_{oc} and I_{sc} can be enhanced by integrating different NGs in serial and parallel connection modes, respectively. Figure 4 displays that the generated V_{oc} of NG was not affected by increasing the driving frequency from 2 to 4 Hz, which shows that the generated V_{oc} exhibited high

stability, demonstrating that the NG made from BaTiO₃ nanotubes is very suitable for energy harvesting driven by irregular excitations in our living environment. Besides, we also tested the lifetime of the as-developed NG. (See Figure 5a.) The peak value of generated V_{oc} of NG did not make a significant change after 3 days (1200 cycles per day). Under periodic external mechanical deformation by biomechanical movements from fist of human body, the output power of an enlarged NG (1.5 \times 4 cm) is sufficient to drive a LCD screen. (See Figure 5b and the video in the Supporting Information.) An LCD is a nonpolar device that can be driven directly by ac power as long as its output potential exceeds a threshold value. The LCD screen used for the test was taken from a Sharp calculator; a proper connection combination was chosen to get an output of number “6” at the front panel. The LCD screen was directly connected to the NG without involvement of any external sources or measurement meters. Figure 5b shows two

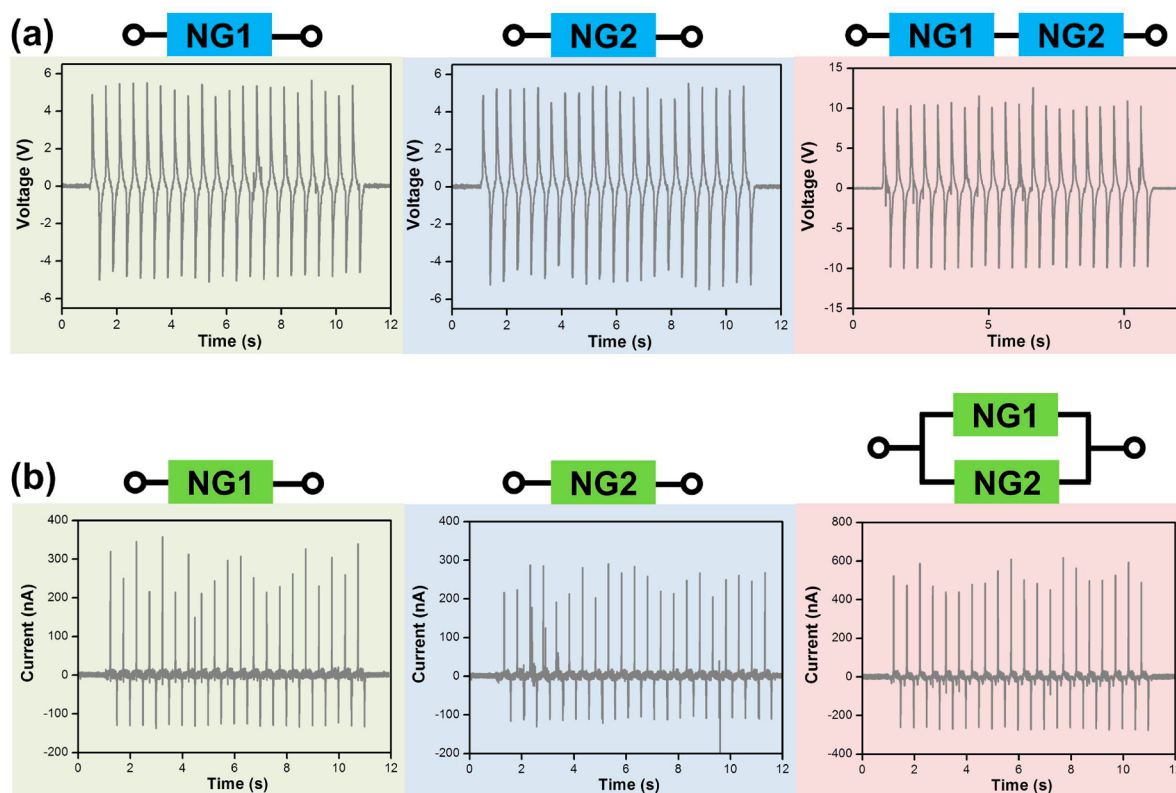


Figure 3. (a) Generated V_{oc} of the separated and serial-connected NGs under a compress stress of 1 MPa. (b) Generated I_{sc} of the separated and parallel-connected NGs under a compress stress of 1 MPa.

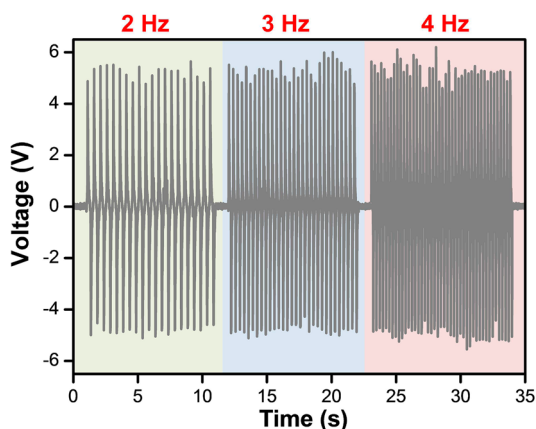


Figure 4. Generated V_{oc} of the as-prepared NG under the same compress stress of 1 MPa but at different frequency of 2, 3, and 4 Hz.

stages taken for a full cycle driving of a LCD by the NG, showing the LCD blinking corresponding to each ac output peak of the NG. The power output at each hit on the NG was able to drive the LCD. (See the video in the Supporting Information.) Figure 5c shows that the nanogenerator was highly transparent, stretchable, and flexible, which exhibits great advantages in the applications of commercial portable devices.

There are several novelties of the BaTiO₃ nanotubes/PDMS composite-based NG. First, a massive production of BaTiO₃ nanotubes through the hydrothermal method enables us the fabrication of NG at a large scale. Second, the electric field can effectively pole random piezoelectric domains to one direction due to the ferroelectricity of BaTiO₃ nanotubes. This simplifies the fabrication procedures of NG. Third, the lead-free NG

solves the problem of using piezoelectric materials with toxic elements. Fourth, the NG keeps the transparent property but with a higher output power as compared to the previously reported BaTiO₃-based NGs. Fifth, the as-prepared NG shows the high flexibility and long stability due to the presence of PDMS.

In summary, we have demonstrated a flexible and transparent piezoelectric NG by using the BaTiO₃ nanotubes/PDMS composite. The output voltage and current of the fabricated NG are up to 5.5 V and 350 nA under a stress of 1 MPa, respectively. The performance of the NG can be enhanced by increasing the concentration of BaTiO₃ nanotubes in the PDMS matrix. An LCD can be directly driven by the NG. This is a practical and versatile technology with the potential for organic electronic and optoelectronic device applications.

EXPERIMENTAL SECTION

Synthesis of BaTiO₃ Nanotubes. 0.25 g TiO₂ nanoparticles (P25, Aldrich) and 0.65 g BaCl₂ (99.9%, Aldrich) were added to 20 mL of 10 M NaOH aqueous solution and then transferred to a 25 mL Teflon-lined stainless-steel autoclave. The sealed autoclave was heated in an oven at 200 °C for 72 h and then cooled in air. To obtain pure BaTiO₃ nanotubes, the solution was subjected to cycles of centrifugation/wash; centrifugation was conducted at 6000 rpm for 20 min, and deionized water (20 × 3 mL) was used to wash the pellets.

Nanogenerator Fabrication. First, the PS substrate was deposited with Au/Cr to serve as a bottom electrode. The BaTiO₃ nanotubes and PDMS solution were mixed together at different ratios of 1, 2, 3, and 4 wt % then deposited onto the Au/Cr coated PS substrate using a spin-coating process (200 rpm, 30 s). Subsequently the device was deposited by Au/Cr

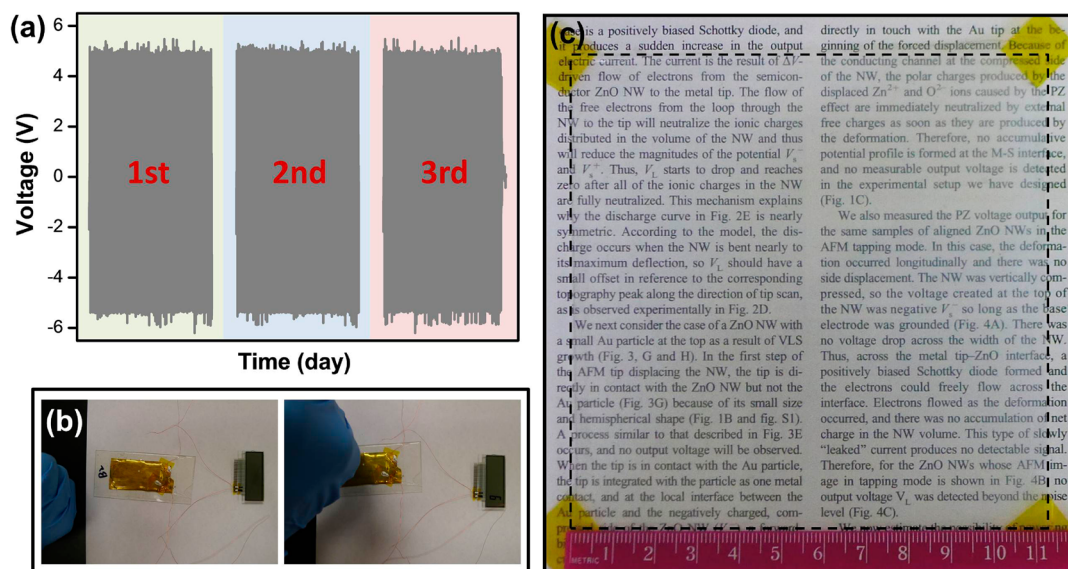


Figure 5. (a) Stability of the as-prepared NG was tested under a compress stress of 1 MPa at different days of operation (1200 cycles per day). (b) Commercial LCD was powered by the as-prepared NG under periodic external mechanical deformation by biomechanical movements from fist of human body. (c) Large-area NG with transparent property was fabricated over 11 cm \times 11 cm in size (dashed line indicates the frame).

again to serve as the top electrode. The Cu wires were attached to the electrodes by means of silver (Ag) paste. Finally, an additional layer of PDMS was coated over the device to keep the nanogenerator robust under the mechanical stress or deformation. The thickness of the BaTiO₃ nanotubes/PDMS composite was \sim 300 μ m. Before the characterization of the output voltage and current signals, the NG was poled at ambient temperature by applying an electric field of 80 kV/cm for 12 h.

Characterization. An FEI Tecnai-G2-F30 TEM was used to measure the size and shape of the BaTiO₃ nanotubes. A LEO 1550 field-emission SEM was used to measure the thickness of BaTiO₃ nanotubes/PDMS composite. An Oxford Inca EDX system was used to determine the compositions of the BaTiO₃ nanotubes. Raman spectrum was recorded using a Nicolet Almega dispersive Raman spectrometer. The output signal of the nanogenerator was measured using a low-noise voltage preamplifier (Stanford Research System model SR560) and a low-noise current preamplifier (Stanford Research System model SR570). The simulation of the piezopotential was conducted by COMSOL Multiphysics version 3.5a. Figure S1c of the Supporting Information gives an example of a single BaTiO₃ nanowire in PDMS under strain. The dimension of the nanowire is 4 μ m in length and 10 nm in diameter, which is similar to the as-prepared nanotube. The PDMS surrounding is 1 μ m in transverse direction and 8 μ m in longitudinal direction. Deformation of the whole geometry is set as 1 μ m compression in longitudinal direction. Figure 2c is the calculated result of the BaTiO₃ nanotubes/PDMS composite-based NG. The simulation is based on a three-layer structure composed of a top PDMS (300 μ m), a layer of BaTiO₃ (300 μ m), and a bottom PS substrate (500 μ m). The calculated piezopotential was expressed as the rainbow color range in the diagram.

■ ASSOCIATED CONTENT

Supporting Information

HRTEM image, XRD, and EDX spectrum of BaTiO₃ nanotubes, COMSOL simulation result of single BaTiO₃ nanowire, effects of poling, applied forces, and weight

(c) is a positively biased Schottky diode, and produces a sudden increase in the output current. The current is the result of the driven flow of electrons from the semiconductor ZnO NW to the metal tip. The flow of the free electrons from the loop through the NW to the tip will neutralize the ionic charges distributed in the volume of the NW and thus will reduce the magnitudes of the potential V_1^+ and V_1^- . Thus, V_1^+ starts to drop and reaches zero after all of the ionic charges in the NW are fully neutralized. This mechanism explains why the discharge curve in Fig. 2E is nearly symmetric. According to the model, the discharge occurs when the NW is bent nearly to its maximum deflection, so V_1^+ should have a small offset in reference to the corresponding topography peak along the direction of tip scan, as observed experimentally in Fig. 2D.

We next consider the case of a ZnO NW with a small Au particle at the top as a result of VLS growth (Fig. 3, G and H). In the first step of the AFM tip displacing the NW, the tip is directly in contact with the ZnO NW but not the Au particle (Fig. 3G) because of its small size and hemispherical shape (Fig. 1B and fig. S1). A process similar to that described in Fig. 3E when the tip is in contact with the Au particle, the tip is integrated with the particle as one metal contact, and at the local interface between the particle and the negatively charged, com-

directly in touch with the Au tip at the beginning of the forced displacement. Because of the conducting channel at the contact point of the NW, the polar charges produced by the displaced Zn²⁺ and O²⁻ ions caused by the PZ effect are immediately neutralized by external free charges as soon as they are produced by the deformation. Therefore, no accumulative potential profile is formed at the M-S interface, and no measurable output voltage is detected in the experimental setup we have designed (Fig. 1C).

We also measured the PZ voltage output for the same samples of aligned ZnO NWs in the AFM tapping mode. In this case, the deformation occurred longitudinally and there was no side displacement. The NW was vertically compressed, so the voltage created at the top of the NW was negative V_1^- , so long as the base electrode was grounded (Fig. 4A). There was no voltage drop across the width of the NW. Thus, across the metal tip-ZnO interface, a positively biased Schottky diode formed and the electrons could freely flow across the interface. Electrons flowed as the deformation occurred, and there was no accumulation of net charge in the NW volume. This type of slowly "leaked" current produces no detectable signal. Therefore, for the ZnO NWs whose AFM image in tapping mode is shown in Fig. 4B no output voltage V_1 was detected beyond the noise level (Fig. 4C).

percentages of BaTiO₃ nanotubes/PDMS on NG electric output, and video showing lighting of an LCD powered by a nanogenerator. This material is available free of charge via the Internet at <http://pubs.acs.org>.

■ AUTHOR INFORMATION

Corresponding Author

*E-mail: zlwang@gatech.edu.

Notes

The authors declare no competing financial interest.

■ ACKNOWLEDGMENTS

This work was supported by Airforce, MURI, U.S. Department of Energy, Office of Basic Energy Sciences (DE-FG02-07ER46394), NSF (CMMI 0403671), Taiwan (NSC 101-2917-I-564-029), National Institute For Materials, Japan (Agreement DTD 1 July 2008), and the Knowledge Innovation Program of the Chinese Academy of Sciences (KJCX2-YW-M13).

■ REFERENCES

- (1) Tian, B.; Zheng, X.; Kempa, T. J.; Fang, Y.; Yu, N.; Yu, G.; Huang, J.; Lieber, C. M. Coaxial Silicon Nanowires as Solar Cells and Nanoelectronic Power Sources. *Nature* **2007**, *449*, 885–890.
- (2) Qin, Y.; Wang, X. D.; Wang, Z. L. Microfibre–Nanowire Hybrid Structure for Energy Scavenging. *Nature* **2008**, *451*, 809–813.
- (3) Yang, Y.; Guo, W.; Pradel, K. C.; Zhu, G.; Zhou, Y.; Zhang, Y.; Hu, Y.; Lin, L.; Wang, Z. L. Pyroelectric Nanogenerators for Harvesting Thermoelectric Energy. *Nano Lett.* **2012**, *12*, 2833–2838.
- (4) Xu, S.; Qin, Y.; Xu, C.; Wei, Y.; Yang, R.; Wang, Z. L. Self-Powered Nanowire Devices. *Nat. Nanotechnol.* **2010**, *5*, 366–373.
- (5) Chen, C.-Y.; Zhu, G.; Hu, Y.; Yu, J.-W.; Song, J.; Cheng, K.-Y.; Peng, L.-H.; Chou, L.-J.; Wang, Z. L. Gallium Nitride Nanowire Based Nanogenerators and Light-Emitting Diodes. *ACS Nano* **2012**, *6*, 5687–5692.
- (6) Hu, Y.; Zhang, Y.; Xu, C.; Zhu, G.; Wang, Z. L. High-Output Nanogenerator by Rational Unipolar Assembly of Conical Nanowires and Its Application for Driving a Small Liquid Crystal Display. *Nano Lett.* **2010**, *11*, 2572–2577.

- (7) Hu, Y.; Zhang, Y.; Xu, C.; Lin, L.; Snyder, R. L.; Wang, Z. L. Self-Powered System with Wireless Data Transmission. *Nano Lett.* **2011**, *11*, 2572–2577.
- (8) Yang, Q.; Guo, X.; Wang, W.; Zhang, Y.; Xu, S.; Lien, D. H.; Wang, Z. L. Enhancing Sensitivity of a Single ZnO Micro-/Nanowire Photodetector by Piezo-phototronic Effect. *ACS Nano* **2010**, *4*, 6285–6291.
- (9) Wang, Z. L.; Song, J. H. Piezoelectric Nanogenerators Based on Zinc Oxide Nanowire Arrays. *Science* **2006**, *312*, 242–246.
- (10) Karanth, D.; Fu, H. Large Electromechanical Response in ZnO and Its Microscopic Origin. *Phys. Rev. B* **2005**, *72*, 064116.
- (11) Fu, H.; Cohen, R. E. Polarization Rotation Mechanism for Ultrahigh Electromechanical Response in Single-Crystal Piezoelectrics. *Nature* **2000**, *403*, 281–283.
- (12) Hernandez, B. A.; Chang, K. S.; Fisher, E. R.; Dorhout, P. K. Sol-Gel Template Synthesis and Characterization of BaTiO₃ and PbTiO₃ Nanotubes. *Chem. Mater.* **2002**, *14*, 480–482.
- (13) Luo, Y.; Szafraniak, I.; Zakharov, N. D.; Nagarajan, V.; Steinhart, M.; Wehrspohn, R. B.; Wendorff, J. H.; Ramesh, R.; Alexe, M. Nanoshell Tubes of Ferroelectric Lead Zirconate Titanate and Barium Titanate. *Appl. Phys. Lett.* **2003**, *83*, 440–442.
- (14) Scott, J. F. Applications of Modern Ferroelectrics. *Science* **2007**, *315*, 954–959.
- (15) Saito, Y.; Takao, H.; Tani, T.; Nonoyama, T.; Takatori, K.; Homma, T.; Nagaya, T.; Nakamura, M. Lead-Free Piezoceramics. *Nature* **2004**, *432*, 84–87.
- (16) Chen, X.; Xu, S.; Yao, N.; Shi, Y. 1.6 V Nanogenerator for Mechanical Energy Harvesting Using PZT Nanofibers. *Nano Lett.* **2010**, *10*, 2133–2137.
- (17) Xu, S.; Hansen, B. J.; Wang, Z. L. Piezoelectric-Nanowire-Enabled Power Source for Driving Wireless Microelectronics. *Nat. Commun.* **2010**, *1*, 93.
- (18) Cross, L. E. Materials Science: Lead-Free at Last. *Nature* **2004**, *432*, 24–25.
- (19) Park, K.-I.; Xu, S.; Liu, Y.; Hwang, G. T.; Kang, S. J. L.; Wang, Z. L.; Lee, K. J. Piezoelectric BaTiO₃ Thin Film Nanogenerator on Plastic Substrates. *Nano Lett.* **2010**, *10*, 4939–4943.
- (20) Agrawal, R.; Espinosa, H. D. Giant Piezoelectric Size Effects in Zinc Oxide and Gallium Nitride Nanowires. A First Principles Investigation. *Nano Lett.* **2011**, *11*, 786–790.
- (21) Majdoub, M. S.; Sharma, P.; Cagin, T. Enhanced Size-Dependent Piezoelectricity and Elasticity in Nanostructures Due to the Flexoelectric Effect. *Phys. Rev. B* **2008**, *77*, 125424.
- (22) Bühlmann, S.; Dwir, B.; Baborowski, J.; Murali, P. Size Effect in Mesoscopic Epitaxial Ferroelectric Structures: Increase of Piezoelectric Response with Decreasing Feature Size. *Appl. Phys. Lett.* **2002**, *80*, 3195–3197.
- (23) Bavykin, D. V.; Parmon, V. N.; Lapkina, A. A.; Walsh, F. C. The Effect of Hydrothermal Conditions on the Mesoporous Structure of TiO₂ Nanotubes. *J. Mater. Chem.* **2004**, *14*, 3370–3377.
- (24) Yang, Y.; Wang, X.; Sun, C.; Li, L. Structure Study of Single Crystal BaTiO₃ Nanotube Arrays Produced by the Hydrothermal Method. *Nanotechnology* **2009**, *20*, 055709.
- (25) Moreira, M. L.; Mambrini, G. P.; Volanti, D. P.; Leite, E. R.; Orlandi, M. O.; Pizani, P. S.; Mastelaro, V. R.; Paiva-Santos, C. O.; Longo, E.; Varela, J. A. Hydrothermal Microwave: A New Route to Obtain Photoluminescent Crystalline BaTiO₃ Nanoparticles. *Chem. Mater.* **2008**, *20*, 5381–5387.
- (26) Brutchey, R. L.; Morse, D. E. Template-Free, Low-Temperature Synthesis of Crystalline Barium Titanate Nanoparticles under Bio-Inspired Conditions. *Angew. Chem., Int. Ed.* **2006**, *45*, 6564–6566.
- (27) Jung, J. H.; Lee, M.; Hong, J.-I.; Ding, Y.; Chen, C.-Y.; Chou, L.-J.; Wang, Z. L. Lead-Free NaNbO₃ Nanowires for a High Output Piezoelectric Nanogenerator. *ACS Nano* **2011**, *5*, 10041–10046.
- (28) Zhu, G.; Wang, A. C.; Liu, Y.; Zhou, Y.; Wang, Z. L. Functional Electrical Stimulation by Nanogenerator with 58 V Output Voltage. *Nano Lett.* **2012**, *12*, 3086–3090.